Histologic abnormalities associated with gadolinium enhancement on MR in the initial hours of experimental cerebral infarction.

V P Mathews, L H Monsein, C A Pardo and R N Bryan

AJNR Am J Neuroradiol 1994, 15 (3) 573-579
http://www.ajnr.org/content/15/3/573

Histologic Abnormalities Associated with Gadolinium Enhancement on MR in the Initial Hours of Experimental Cerebral Infarction

Vincent P. Mathews, Lee H. Monsein, Carlos A. Pardo, and R. Nick Bryan

PURPOSE: To determine the histologic changes associated with gadopentetate dimeglumine enhancement on MR images in acute focal cerebral ischemia. **METHODS:** In each of two baboons, a microcatheter was used to occlude partially the middle cerebral artery and reduce cerebral blood flow for approximately 3.5 hours. The catheter was then removed allowing reperfusion for approximately 3.5 hours. In two other baboons, cerebral blood flow was completely and irreversibly interrupted by injecting liquid adhesive into the middle cerebral artery. T2-weighted and serial enhanced T1-weighted MR images were obtained. Brain specimens were studied histopathologically. **RESULTS:** In the animals with incomplete and reversible reduction of cerebral blood flow, postcontrast T1-weighted images obtained during the initial 3 hours of ischemia showed focal areas of hypointensity. These areas were enhanced on later images. The areas of signal abnormality were subsequently found to be necrotic and were characterized by neuronal cytolysis and vascular "plugging." In the animals with complete and irreversible interruption of cerebral blood flow, no abnormal signal intensity or enhancement was observed. Histologic abnormalities were milder in these animals. **CONCLUSIONS:** Contrast enhancement on MR images in the initial hours of cerebral ischemia was associated with histologic evidence of tissue necrosis but was not associated with milder ischemic changes.

Index terms: Brain, ischemia; Magnetic resonance, tissue characterization; Pathology; Animal studies; Brain, magnetic resonance

AJNR Am J Neuroradiol 15:573–579, Mar 1994

Several investigators have recently studied the use of gadopentetate dimeglumine–enhanced magnetic resonance (MR) imaging in the evaluation of cerebral infarction (1–7). Enhancement of brain parenchyma is uncommon in the first 6 days after stroke but is almost uniformly present during the subsequent weeks after infarction (3, 4). In one study, early parenchymal enhancement in the first few days after infarction was often seen in patients with minimal or reversible neurologic deficits and was believed to be related to incomplete ischemia (5). In an experimental study, enhancement was not seen within the initial 2 hours of ischemia but was uniformly seen after 16 hours. The areas of enhancement corresponded pathologically to areas of infarction (1). These studies suggest that MR contrast enhancement may have clinical or pathologic significance.

The purpose of this study was to determine the histologic findings associated with the presence or absence of contrast enhancement on MR studies of experimental cerebral ischemia. This pathologic-MR correlative study used baboons and two models of acute focal cerebral ischemia, one in which cerebral blood flow was partially and reversibly reduced and one in which cerebral blood flow was completely and irreversibly interrupted.

Received November 24, 1992; accepted pending revision March 21, 1993; revision received May 28.

Supported in part by the American Society of Neuroradiology's Fellowship in Basic Science Research (to L.H.M.), the Radiological Society of North America's Research and Education Fund (to V.P.M.), and the Fogarty International Fellowship No. 1 F05 TW 04305–01 (to C.A.P.).

From the Division of Neuroradiology, Russell H. Morgan Department of Radiology and Radiological Science (V.P.M., L.H.M., R.N.B.), and Neuropathology Laboratory, Department of Pathology (C.A.P.), Johns Hopkins University School of Medicine, Baltimore, Md.

Address reprint requests to Vincent P. Mathews, MD, Department of Radiology, Bowman Gray School of Medicine of Wake Forest University, Medical Center Blvd, Winston-Salem, NC 27157-1088.

AJNR 15:573–579, Mar 1994 0195-6108/94/1503–0573

Methods

Animal Model

After overnight fasting, four male baboons ranging from 16 to 18 kg in weight were initially anesthetized with intramuscular ketamine hydrochloride (200 mg) followed by intravenous sodium pentobarbital (65 mg/hr). The animals were intubated, paralyzed with intravenous pancuronium bromide (0.04 mg/kg), and placed on a mechanical ventilator. Respiration, blood pressure, and body temperature were monitored and maintained within normal ranges.

Next, 7-F sheaths were placed in both common femoral arteries and the left axillary artery. One femoral sheath and the left axillary sheath were used for radioactive microsphere cerebral blood flow measurements as described previously (8). The other femoral sheath was used for angiography and catheterization of the middle cerebral artery. For digital subtraction angiography, ioxaglate sodium meglumine (Hexabrix, Mallinckrodt, St. Louis, Mo) was injected by hand at varying rates according to vessel size. Image acquisition rate was three frames per second.

In animals 1 and 2 a 7-F tapering to 5-F catheter was positioned in a common carotid artery. A 2.7-F microcatheter (Tracker 18, Target Therapeutics, San Jose, Calif) was passed coaxially through the internal carotid artery into the M2 segment of the middle cerebral artery. The animals were then immediately transferred to the MR instrument. The microcatheter was removed from the first animal 3.3 hours after it was positioned in the middle cerebral artery, and the animal was killed 3.3 hours later. The microcatheter was removed from the second animal 3.5 hours after it was positioned in the middle cerebral artery; the animal was killed 3.6 hours later.

In animals 3 and 4 a 7-F tapering to 5-F catheter was positioned in a common carotid artery. A 2-F microcatheter (Tracker 10, Target Therapeutics) was passed coaxially through the internal carotid artery into the left middle cerebral artery. With the tip of the catheter in the M1 segment of the middle cerebral artery, a mixture of 1.0 mL of N-butyl cyanoacrylate (Tripoint Medical L.P., Raleigh, NC), 500 mg of tantalum powder, and 0.5 mL of iophendylate (Pantopaque; Lafayette Pharmaceutical, Lafayette, Ind) was injected until it was seen exiting the tip of the microcatheter, which was then withdrawn (8). Under fluoroscopy the glue was seen to fill the middle cerebral artery and proximal middle cerebral artery branches and to reflux into the ipsilateral anterior cerebral artery. The animals were then immediately transferred to the MR instrument. Animal 3 was killed 3.5 hours and animal 4 7.7 hours after middle cerebral artery occlusion.

Radioactive microsphere (NEN-Trac; Dupont, NEN Research Products, Boston, Mass) cerebral blood flow measurements were taken before occlusion and after reperfusion in animals 1 and 2 and before and after occlusion in animals 3 and 4 (9).

MR

MR data were obtained with a 1.5-T clinical MR instrument (Signa; GE Medical Systems, Milwaukee, Wis.) and a standard extremity radio frequency coil. Imaging times are listed in Table 1. Multiple spin-echo spin density–weighted 3000/30/1 (repetition time/echo time/excitations) and T2-weighted 3000/100/1 sequences were used to obtain contiguous sections 5 mm thick in the coronal plane. Multiple T1-weighted three-dimensional volume gradient-echo images were obtained using 35/15/1 and a 45° flip angle to allow the acquisition of 1.5-mm sections. Three-dimensional time-of-flight MR angiography was performed with a gradient-echo sequence with the following parameters: 40/5.5/1, 20° flip angle, 18-cm field of view, 128 × 256 matrix, and 28 partitions of a 28-mm slab.

Times of contrast material injection are noted in Table 1. Gadopentetate dimeglumine was injected at a dose of 0.3 mmol/kg.

Pathology

The brain specimens were studied with histopathologic techniques after perfusion fixation. A catheter was passed into the left ventricle, the right atrium was incised, and the aorta was clamped distally to the left subclavian artery. A 10-minute perfusion of phosphate buffered saline (0.1 m, pH 7.4) was followed by 4% paraformaldehyde in phosphate buffered saline for 30 minutes. After perfusion, the brain was removed, fixed in 4% paraformaldehyde for 48 hours, and cut into sections 5 mm thick in a plane similar to that in which the MR images were obtained. The sections were cryoprotected in 20% glycerol for 48 hours and frozen in isopentane at −70° C.

TABLE 1: Sequence of key events (all times in hours after occlusion of middle cerebral artery)

	Reversible Ischemia		Irreversible Ischemia	
	Animal 1	Animal 2	Animal 3	Animal 4
Cerebral blood flow measured	−1.7	−2.0	−4.8	−2.0
Contrast injected	1.0	1.4	1.7	1.9
T1-weighted images	2.7	1.1	−3.6	0.6
	5.6[a]	2.5	2.2	2.2
		3.5[a]	2.9	4.6
		5.3[a]		
Spin density–weighted	2.5	2.6	−3.8	4.0
and T2-weighted images	4.7	4.7	1.7	
	5.4			
Catheters removed	3.3	3.5	NA	NA
Cerebral blood flow measured	3.4	6.8	3.1	5.4
Animals killed and specimens harvested	6.6	7.1	3.5	7.7

Note: NA indicates not applicable.

[a] Contrast enhancement.

Serial frozen sections 20 μm thick were obtained and stained with cresyl-violet, hematoxylin-eosin, and luxol-fast blue/hematoxylin-eosin. The magnitude and topographical distribution of normal, ischemic, and necrotic neurons were determined by analysis of the cresyl-violet- and hematoxylin-eosin-stained sections according to the histologic criteria established previously for these neuronal changes (10, 11). Cytologic criteria for necrotic cells included cytolysis, vacuolation, or nuclear condensation. Ischemic cells demonstrated milder abnormalities, including cellular swelling without lysis and nuclear distortion without pyknosis. The extent and magnitude of myelin changes were established by analysis of luxol-fast blue/hematoxylin-eosin-stained sections. Neuronal damage and myelin breakdown were studied topographically by analysis of the sections with a computerized plotting system for mapping necrotic and ischemic neurons.

Results

Animal Model

Digital subtraction angiography showed a patent middle cerebral artery, and radioactive microsphere cerebral blood flow measurements demonstrated normal cerebral blood flow (40–60 mL/100 g/min) before occlusion in all four animals. Flow in the ipsilateral middle cerebral artery was not visualized with digital subtraction angiography or MR angiography after temporary occlusion with a catheter in animals 1 and 2. Radioactive microsphere cerebral blood flow measurements are unreliable during temporary occlusion, because radioactive microsphere can lodge around the catheter in the vessel and then migrate distally when the catheter is removed. We have previously observed with H_2O^{15} positron emission tomography that there is incomplete reduction in cerebral blood flow in the basal ganglia during occlusion of the middle cerebral artery with an endovascular catheter (our unpublished data). After removal of the catheter, the middle cerebral artery was again visualized with MR angiography, and radioactive microsphere cerebral blood flow measurements confirmed restoration of normal cerebral blood flow to the ipsilateral hemisphere.

Flow in the middle cerebral artery was not visualized after injection of glue in animals 3 and 4 with digital subtraction or MR angiography, and radioactive microsphere cerebral blood flow measurements demonstrated no measurable cerebral blood flow in the distribution of the middle cerebral artery.

MR

In animal 1, initial T1-weighted images (Fig 1A) demonstrated patchy decreased signal in the region of the external capsule and putamen which densely enhanced on later T1-weighted images (Fig 1B). There were corresponding areas of increased signal on the second and third spin density–weighted and T2-weighted studies (Fig 1C), but no abnormal signal was seen on these sequences initially.

In animal 2, the initial T1-weighted images were normal. The second T1-weighted study demonstrated a focal area of decreased signal in the head of the right caudate nucleus. This area was densely enhanced on subsequent T1-weighted images. There was progressively abnormal hyperintensity in this region on spin density–weighted and T2-weighted imaging sequences.

In animals 3 and 4, T1-weighted images demonstrated no abnormalities of the brain parenchyma. Spin density–weighted and T2-weighted images were normal (Fig 2A).

Pathology

In animals 1 and 2, well-defined areas of necrosis without hemorrhage were observed grossly and microscopically in the caudate and putamen. The necrotic regions were well established and were characterized by shrinkage or disintegration of neurons or ghost neurons. They were surrounded by areas containing neurons with variable degrees of ischemic injury (Figs 1D–1F). These areas of necrosis corresponded to the areas of contrast enhancement on MR images. Within areas of necrosis, blood vessels were filled with solid casts of red blood cells in which individual red cells could not readily be delineated.

In animals 3 and 4, the histologic changes (Figs 2C–2E) were far less severe than in animals 1 and 2. There were widespread early and intermediate stages of ischemic injury in the basal ganglia and cortex with scattered, nonconfluent small foci of necrosis. Blood vessels throughout the ipsilateral hemisphere were filled with strings of red blood cells that were individually identifiable.

Discussion

Our study describes histologic changes secondary to ischemia and relates these changes to the presence or absence of contrast enhancement on MR. A previous animal study of gadopentetate

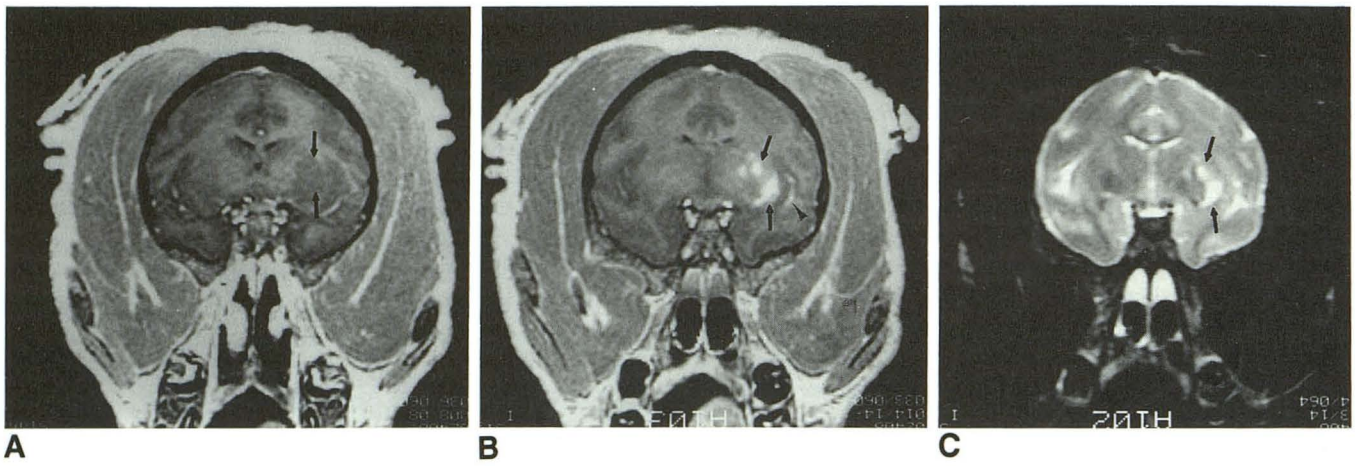
A
B
C

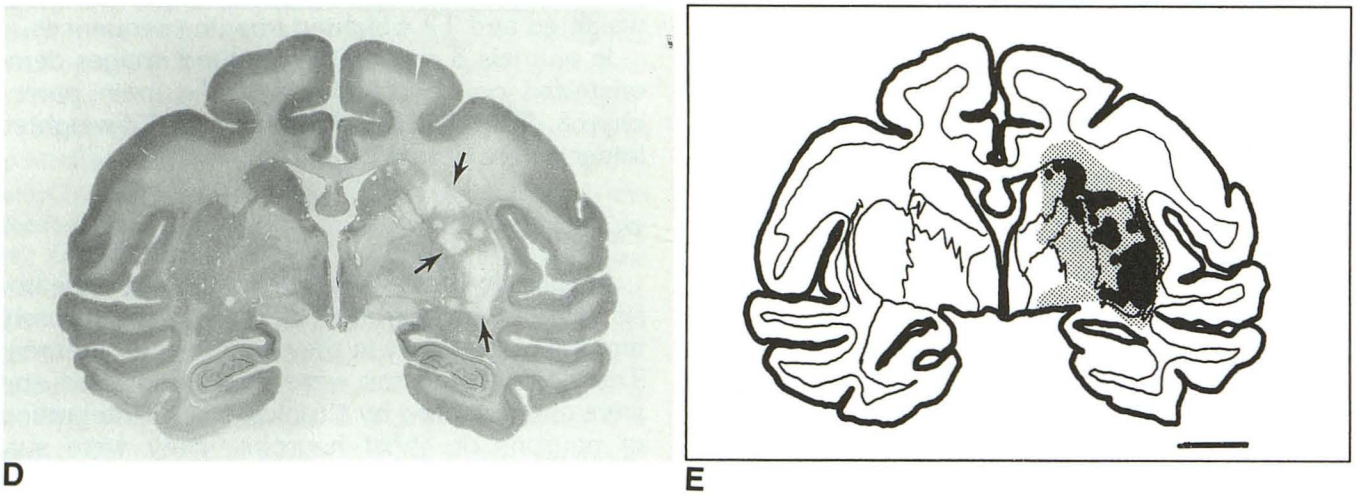
D
E

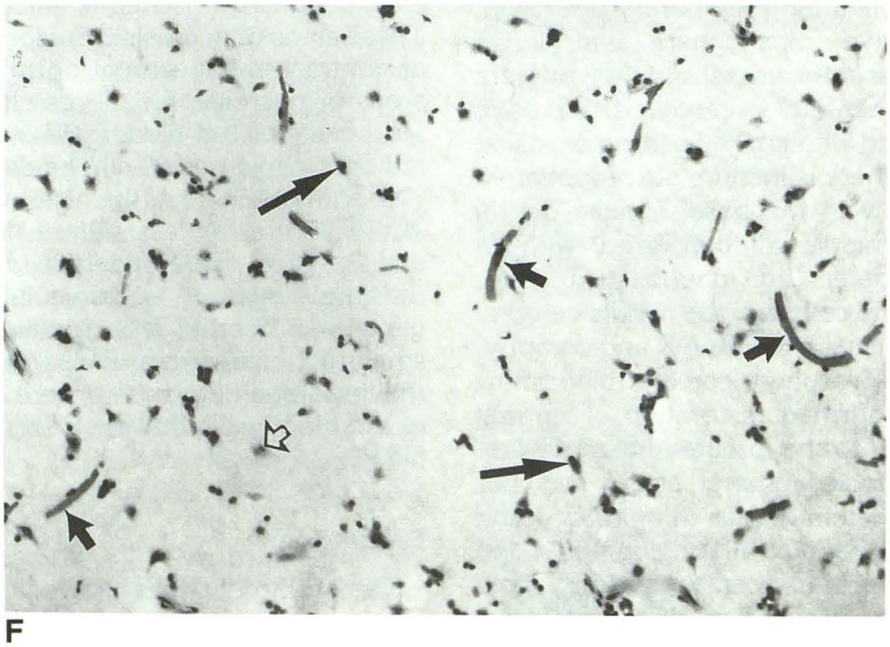
F

dimeglumine–enhanced MR imaging of cerebral ischemia described parenchymal enhancement in areas of infarction but did not describe in detail the histology in their animals (1). One clinical study reported that parenchymal enhancement in the first 3 days after infarction was associated with minimal or reversible neurologic deficits and appeared to be related to incomplete ischemia (5). These studies suggest that parenchymal enhancement may have both pathologic and clinical implications.

The parenchymal enhancement noted in our experiments occurred only in the animals with incomplete and reversible interruption of cerebral blood flow. These areas of contrast enhancement corresponded to confluent areas of necrosis pathologically. Areas of ischemic cellular changes without confluent necrosis were not enhanced in either model of ischemia. Contrast medium could not be delivered to this injured tissue in the animals with complete and irreversible reduction of cerebral blood flow but could be delivered to ischemic tissue in the other two animals. This fact indicates that during the early hours of cerebral ischemia the blood-brain barrier was intact in areas of milder ischemic changes but not in necrotic areas. MR was insensitive in detecting the milder tissue injury: neither parenchymal enhancement nor other signal abnormality was seen in these locations.

In the animals with incomplete and reversible reduction of cerebral blood flow, enhancement of areas of infarction was not seen until 2.1 and 4.6 hours after injection. Contrast enhancement on delayed but not on immediate imaging has been described in brain neoplasms (12, 13) but has not to our knowledge been described in association with cerebral infarction. Delayed enhancement is possible; 6.5% to 12% of the injected dose of gadolinium remains in the plasma at 1 to 2 hours after injection (14). The use of 0.3 mmol/kg gadopentetate dimeglumine, which is three times the usual clinical dose, was important to ensure that an adequate amount of contrast agent remained in the plasma so that delayed enhancement could occur. Alternatively, multiple contrast injections could have been performed.

Early parenchymal contrast enhancement has been relatively infrequent in clinical studies of ischemia (2–7), probably because impairment of perfusion of infarcted tissue can occur even if large vessel blood flow is restored (15–17). The microcirculatory obstruction that occurs after temporary cerebral ischemia has been termed the "no reflow" phenomenon (16). A number of initiating mechanisms have been implicated in this phenomenon, including swelling of perivascular glia (15), hemoconcentration (18, 19), and white blood cell adherence to endothelium (17).

Our study suggests another possible mechanism for the no-reflow phenomenon. Within areas of necrosis, blood vessels were filled with solid casts of red blood cells in which individual red blood cells could not readily be delineated. This phenomenon, which we termed microvascular "plugging," contrasts with a phenomenon we termed microvascular "stasis," in which blood vessels are filled with strings of red blood cells that are individually identifiable. Microvascular stasis is typical for tissue in which perfusion fixation is not done (as when immersion fixation is used) or is inadequate because of compromise in delivery of the fixative (as in animals 3 and 4 in which vessels were occluded with glue). No stasis or plugging was noted in perinecrotic ischemic areas and nonischemic brain. Because we were not able to remove the microvascular plugs seen in our animals with perfusion fixation, we presume that they could cause microcirculatory obstruction. We are not aware of a description of the specific type of microvasculature plugs observed in our experiments. Because we observed

Fig. 1. Animal 1.

A, T1-weighted image at 2.5 hours after occlusion (1.5 hours after injection of contrast) demonstrates patchy areas of decreased signal in the external capsule and putamen (*arrows*).

B, T1-weighted image at 5.6 hours after occlusion (4.6 hours after injection of contrast, 2.3 hours after the catheter was removed) demonstrates enhancement of the regions that had decreased signal on earlier T1-weighted images (*arrows*). Also note the subtle intravascular or pial enhancement in the Sylvian fissure on the side of the infarct (*arrowhead*).

C, T2-weighted image at 5.4 hours after occlusion (2.1 hours after removal of the catheter) demonstrates corresponding areas of increased signal (*arrows*).

D, Histologic preparation (cresyl-violet) demonstrates extensive areas of necrosis (absent staining, *arrows*) matching the areas of abnormal MR signal intensity and enhancement.

E, Computerized plotting of microscopic changes (map) demonstrates extensive necrotic (*black*) changes in the external capsule and putamen, matching the areas of abnormal MR signal intensity and enhancement. More widespread areas of ischemia (*stippled*) are also seen.

F, Histologic appearance of necrosis in the basal ganglia. Note shrinkage (*long arrows*) and disintegration (*open arrow*) of neurons and plugging of blood vessels (*short arrows*) (hematoxylin-eosin 200X).

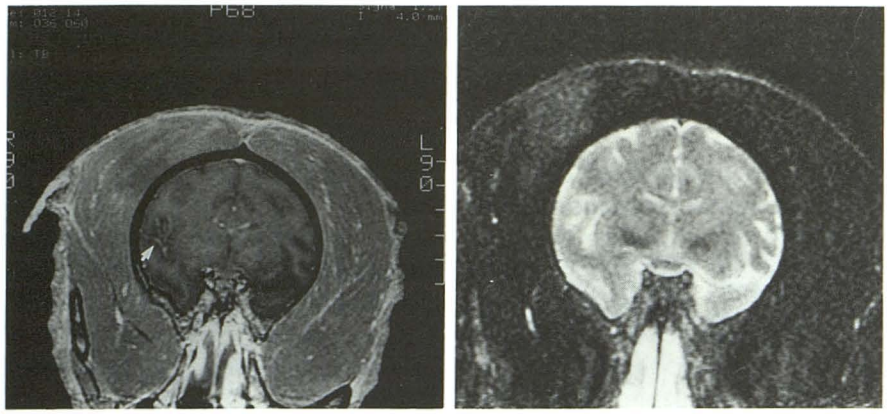

A

B

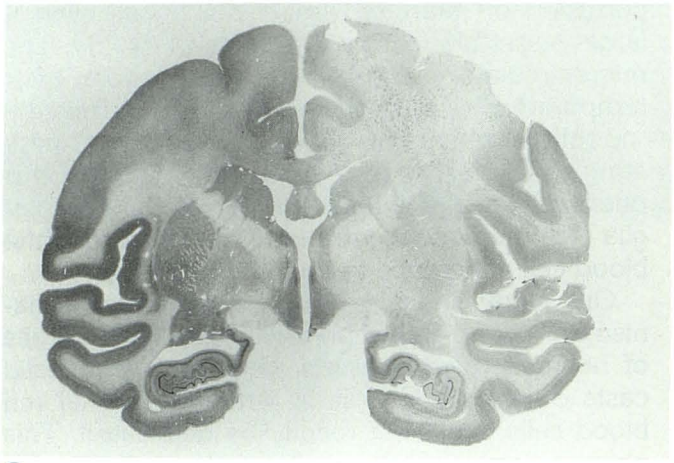

C

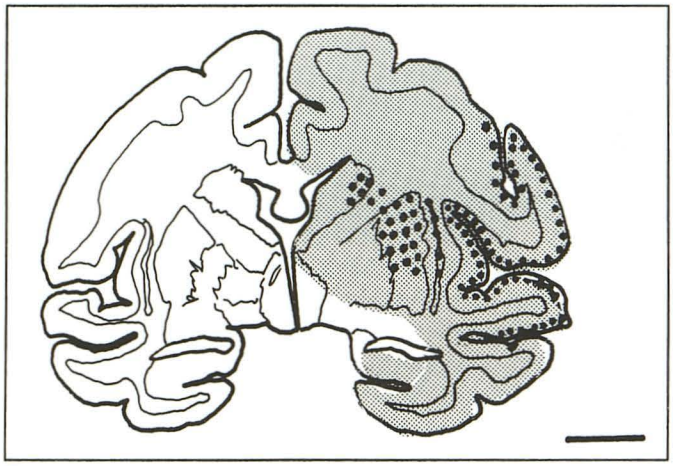

D

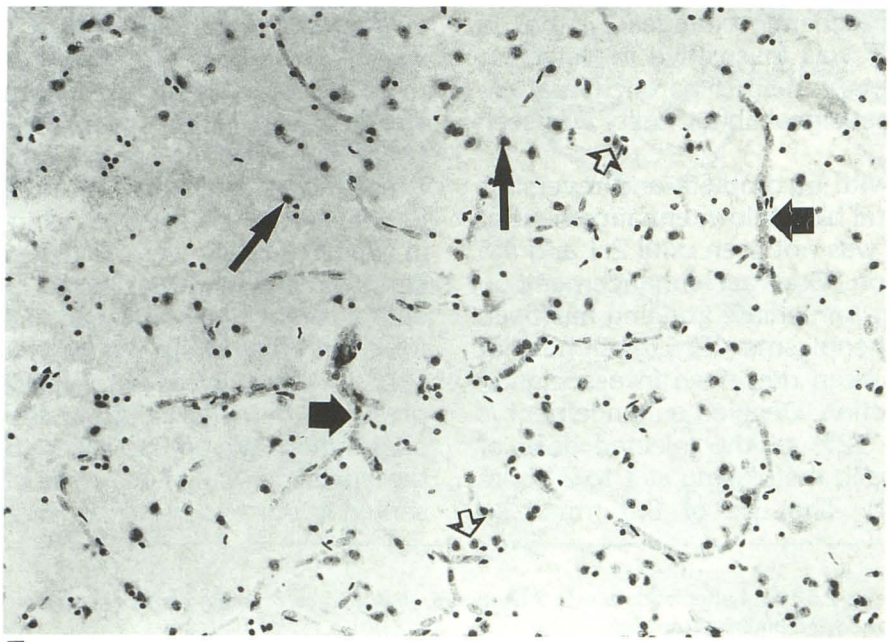

E

Fig. 2. Animal 3.

A, T1-weighted image at 2.8 hours after occlusion (1.1 hours after injection of contrast) demonstrates no parenchymal abnormalities. Note the normal hyperintensity of vessels on the gradient-echo image on the right (*arrow*) and the absence of vascular hyperintensity in the ischemic left hemisphere.

B, T2-weighted image at 1.4 hours after occlusion of middle cerebral artery is normal.

C, Histologic preparation (cresyl-violet) demonstrates ischemic changes (pallor) in the distribution of the middle cerebral artery.

D, Computerized plotting of microscopic changes (map) demonstrates widespread ischemic changes (*stippled*) affecting the cortical and basal ganglia regions. Multiple foci (*black dots*) of neurons with necrotic changes were also present in the frontotemporal and insular cortices and external portion of the caudate and putamen. No confluent cores of necrotic tissue were seen as with animals 1 and 2.

E, Ischemic area in the basal ganglia. Neurons show variable stages of ischemic injury (*thin arrows*) but several neurons are morphologically normal (*open arrows*). Blood vessels display "stasis" (*wide arrows*) (hematoxylin-eosin 200X).

contrast enhancement in areas of necrosis, the blood-brain barrier abnormality is presumed to have developed while contrast was being delivered to the tissue before the formation of the microvascular plugs. Further studies should be performed to determine whether the development of a no-reflow phenomenon can prevent enhancement of ischemic tissue when contrast is administered at times later than those in our experiments.

Comparison of our experimental results with those of clinical studies is limited by the fact that we used higher doses of gadopentetate dimeglumine than were used in these other studies. Large doses of paramagnetic contrast agents have been used to increase the sensitivity for detecting brain neoplasms in humans (20) and might improve detection of blood-brain barrier abnormalities in clinical stroke as well.

In summary, this study demonstrated that contrast enhancement on MR images in the initial hours of cerebral ischemia was associated with histologic evidence of tissue necrosis (cytolysis, vacuolation, or nuclear condensation) but was not associated with milder ischemic changes (cellular swelling without lysis and nuclear distortion without pyknosis). Severe pathologic changes occurred in the first 7 hours of ischemia when cerebral blood flow was partially and reversibly reduced but not when cerebral blood flow was completely and irreversibly interrupted.

Acknowledgments

The investigators acknowledge the significant contributions of Michael A. Samphilipo, Hugh Wall, and Alex Y. Razumovsky in performing the experiments. The map of neuronal damage and myelin breakdown was generated by using the neuromap image analysis system developed by Mark Molliver and Cathy Fleischman of the Neuropathology Laboratory at Johns Hopkins University School of Medicine.

References

1. McNamara MT, Brant-Zawadzki M, Berry I, et al. Acute experimental cerebral ischemia: MR enhancement using Gd-DTPA. *Radiology* 1986;158:701–705
2. Virapongse C, Mancuso A, Quisling R. Human brain infarcts: Gd-DTPA-enhanced MR imaging. *Radiology* 1986;161:785–794
3. Imakita S, Nishimura T, Yamada N, et al. Magnetic resonance imaging of cerebral infarction: time course of Gd-DTPA enhancement and CT comparison. *Neuroradiology* 1988;30:372–378
4. Elster AD, Moody DM. Early cerebral infarction: gadopentetate dimeglumine enhancement. *Radiology* 1990;177:627–632
5. Crain MR, Yuh WTC, Greene GM, et al. Cerebral ischemia: evaluation with contrast-enhanced MR imaging. *AJNR Am J Neuroradiol* 1991;12:631–639
6. Elster AD. MR contrast enhancement in brainstem and deep cerebral infarction. *AJNR Am J Neuroradiol* 1991;12:1127–1132
7. Sato A, Takahashi S, Soma Y, et al. Cerebral infarction: early detection by means of contrast-enhanced cerebral arteries at MR imaging. *Radiology* 1991;178:433–439
8. Monsein LH, Mathews VP, Barker PB, Pardo CA, Bryan RN. Serial MR imaging and proton spectroscopy in a non-human primate model of irreversible regional cerebral ischemia. *AJNR Am J Neuroradiol* (in press)
9. Heymann MA, Payne BD, Hoffman JI, Rudolph AM. Blood flow measurements with radionuclide-labeled particles. *Prog Cardiovasc Dis* 1977;20:55–79
10. Garcia JH, Lossinsky AS, Kauffman FC, Conger KA. Neuronal ischemic injury: light microscopy, ultrastructure and biochemistry. *Acta Neuropathol (Berl)* 1978;43:85–95
11. Eke A, Conger KA, Anderson M, Garcia JH. Histologic assessment of neurons in rat models of cerebral ischemia. *Stroke* 1990;21:299–304
12. Russell EJ, Geremia GK, Johnson CE, et al. Multiple cerebral metastases: detectability with Gd-DTPA-enhanced MR imaging. *Radiology* 1987;165:609–617
13. Schörner W, Laniado M, Niendorf HP, Schubert C, Felix R. Time-dependent changes in image contrast in brain tumors after gadolinium-DTPA. *AJNR Am J Neuroradiol* 1986;7:1013–1020
14. Weinmann HJ, Laniado M, Mützel W. Pharmacokinetics of GdDTPA/dimeglumine after intravenous injection into healthy volunteers. *Physiol Chem Phys Med NMR* 1984;16:167–172
15. Ames A III, Wright RL, Kowada M, Thurston JM, Majno G. Cerebral ischemia. II. The no-reflow phenomenon. *Am J Pathol* 1968;52:437–453
16. Kågström E, Smith M-L, Siesjö BK. Recirculation in the rat brain following incomplete ischemia. *J Cereb Blood Flow Metab* 1983;3:183–192
17. Mori E, del Zoppo GJ, Chambers JD, Copeland BR, Arfors KE. Inhibition of polymorphonuclear leukocyte adherence suppresses no-reflow after focal cerebral ischemia in baboons. *Stroke* 1992;23:712–718
18. Fischer EG, Ames A III. Studies on mechanisms of impairment of cerebral circulation following ischemia: effect of hemodilution and perfusion pressure. *Stroke* 1972;3:538–542
19. Fischer EG, Ames A III, Lorenzo AV. Cerebral blood flow immediately following brief circulatory stasis. *Stroke* 1979;10:423–427
20. Yuh WTC, Fisher DJ, Engelken JD, et al. MR evaluation of CNS tumors: dose comparison study with gadopentetate dimeglumine and gadoteridol. *Radiology* 1991;180:485–491